Scientific Research Publishing

Engineering, 2026, 18(11), 481-489
https://www.scirp.org/journal/eng
ISSN Online: 1947-394X
ISSN Print: 1947-3931

Experimental Study on the Basic Mechanical Properties and Stress-Strain Relationship of Basalt-Fiber-Reinforced Recycled Aggregate Concrete

Lucen Hao

College of Railway Engineering, Guangzhou Railway Polytechnic, Guangzhou, China
Email: haolucen@gtxy.edu.cn

How to cite this paper: Hao, L.C. (2026) Experimental Study on the Basic Mechanical Properties and Stress-Strain Relationship of Basalt-Fiber-Reinforced Recycled Aggregate Concrete. *Engineering*, **18**, 481-489.
https://doi.org/10.4236/eng.2026.1811026

Received: September 10, 2026
Accepted: November 6, 2026
Published: November 9, 2026

Copyright © 2026 by author(s) and Scientific Research Publishing Inc.
This work is licensed under the Creative Commons Attribution International License (CC BY 4.0).
http://creativecommons.org/licenses/by/4.0/

Open Access

Abstract

Basalt-fiber-reinforced recycled aggregate concrete (BFRAC) with fiber dosages of 0, 3, and 6 kg/m^3 was investigated using cube compressive, splitting tensile, flexural, and axial compressive tests. The compressive stress-strain responses were also examined and fitted using a piecewise constitutive model. The reported strength values decreased at 3 kg/m^3 and increased at 6 kg/m^3 relative to the fiber-free mixture. At 6 kg/m^3, the reported splitting tensile and flexural strengths were numerically higher by 11.0% and 10.5%, respectively. The reported peak strain and strain at 50% of peak stress on the descending branch increased by 8.7% and 84.3%, respectively. These observations suggest greater deformation capacity under the reported test conditions. The strength differences are treated as descriptive because their reliability requires verification against specimen and batch variability.

Keywords

Basalt Fibers, Recycled Aggregate Concrete, Mechanical Properties, Stress-Strain Relationship

1. Introduction

Reusing waste concrete as recycled aggregate offers a route to conserving natural aggregates and improving material resource efficiency. Recent studies have explored combined modification of recycled aggregate concrete (RAC) with basalt fibers, copper slag, and ground granulated blast furnace slag [1], and with basalt fibers and volcanic ash [2]. These approaches illustrate the potential of combining

recycled aggregates with fiber reinforcement and supplementary materials. However, the heterogeneous interfacial structure of recycled aggregates can create weak zones within RAC [3], and its mechanical performance remains sensitive to aggregate quality and mixture design [4].

Basalt fibers provide an inorganic reinforcement option for improving crack resistance and deformation capacity. Bao *et al.* [5] compared basalt- and glass-fiber-reinforced RAC and observed benefits in splitting tensile and flexural strength, while the compressive strength of their basalt-fiber mixtures was lower than that of unreinforced RAC. Shi *et al.* [6] examined fracture properties using notched-beam tests and showed that the effect of basalt fibers on fracture energy and crack resistance depends on fiber parameters and the recycled aggregate replacement ratio. Earlier work by Sim *et al.* [7] established the potential of basalt fibers as a strengthening material for concrete structures. More recent uniaxial-compression studies have extended this work to RAC: Guo *et al.* [8] investigated the complete compressive stress-strain response and found that suitable fiber additions can enhance compressive toughness, while Sun *et al.* [9] reported dosage-dependent changes in peak strength and a more gradual descending branch. These findings highlight the need to evaluate strength together with deformation and post-peak behavior.

Despite the expanding literature, the effects of basalt fibers on RAC are not uniform across mixtures. Variations in recycled aggregate characteristics, fiber dosage and dispersion, and matrix composition complicate direct comparisons. Dong *et al.* [10] reported reductions in compressive and splitting tensile strengths for concrete made with recycled earthquake waste, whereas Katkhuda and Shatarat [11] studied chopped basalt fibers together with acid-treated recycled aggregates and reported improved splitting tensile and flexural strengths, with little change in compressive strength. The different aggregate sources and treatment conditions therefore need to be considered when interpreting these results. A systematic assessment of the mechanical properties and stress-strain response under the mixture conditions used in the present study is consequently warranted.

Accordingly, basic mechanical tests were conducted on basalt-fiber-reinforced recycled aggregate concrete with different fiber dosages, including compressive strength, splitting tensile strength, flexural strength, and axial compressive strength, to investigate the effect of basalt fibers on the mechanical properties of RAC. To further clarify the role of basalt fibers in RAC, the stress-strain constitutive relationships of BFRAC with different fiber dosages were also examined.

2. Materials and Test Methods

The cementitious material used in BFRAC was ordinary Portland cement of strength grade 42.5. BFRAC contained two types of aggregate: recycled coarse aggregate (RCA) and natural fine aggregate (FA). The coarse aggregate particle size ranged from 5 to 20 mm. River sand with a fineness modulus of 2.37 was used as the fine aggregate; its properties are listed in **Table 1**. Chopped basalt fibers were

used, as shown in Figure 1, and their properties are listed in Table 2. The BFRAC mixture proportions are given in Table 3.

The recycled coarse aggregate was sourced from Handan, Hebei Province, China, and produced by crushing structural concrete. The RCA was in a saturated-surface-dry (SSD) condition before mixing. Table 1 lists the measured aggregate properties. The water quantity of 196 kg in Table 3 corresponds to SSD aggregate conditions. All solid ingredients, including the basalt fibers for the reinforced mixtures, were premixed for 30 s. Water was then added, and mixing continued for 2 min. The specimens were subjected to standard curing at 20˚C ± 0.5˚C and 95% relative humidity and tested at an age of 28 days.



Figure 1. Chopped basalt fibers.

Table 1. Physical properties of the aggregates.

Property	RCA	FA
Apparent density (g·cm^{-3})	2.45	2.65
Bulk density (g·cm^{-3})	1.17	1.45
Moisture content (%)	1.6	0.8
Water absorption (24 h, %)	5.2	3.6
Crushing index (%)	13.8	-
Loss on ignition (%)	9.2	6.1

Table 2. Physical properties of the basalt fibers.

Length (mm)	Density (kg/m^3)	Tensile strength (MPa)	Elastic modulus (GPa)	Elongation at break	Fiber diameter (μm)
20	2650	4150 - 4800	93 - 110	3.1%	15

Table 3. Concrete mixture proportions (unit: kg).

	Natural aggregate	Recycled aggregate	Sand	Cement	Water	Fiber dosage
Mixture	0	1156	716	326	196	0 3.0 6.0

Three types of specimen geometries were prepared for the tests: (1) 150 mm × 150 mm × 150 mm cubes for compressive-strength and splitting-tensile-strength tests; (2) 100 mm × 100 mm × 400 mm prisms for flexural-strength tests; and (3) 150 mm × 150 mm × 300 mm prisms for axial-compressive-strength tests and determination of the stress-strain constitutive relationship. The mechanical-property tests were conducted in accordance with the Standard for Test Method of Mechanical Properties on Ordinary Concrete [12]. Each dosage was produced in one batch, with three specimens per test, and the result was taken as the average of the three specimens.

Uniaxial compression was conducted with a load-cell capacity of 1000 kN. Loading was applied under actuator-displacement control at a rate of 0.002 mm/s. The LVDTs had a displacement range of ±2.5 mm. The stress-strain responses presented in **Figures 2-4** are dosage-level average results based on three specimens. **Table 5** summarizes the corresponding average characteristic values, and **Table 6** reports one fitted parameter pair for each dosage-level response.

3. Results and Discussion

3.1. Basic Mechanical Properties

Table 4 lists the average mechanical-property results at the three basalt fiber dosages. Relative to 0 kg/m^3, the values at 3 kg/m^3 are numerically lower by 6.6%, 4.4%, 4.2%, and 4.8% for cube compressive, splitting tensile, flexural, and axial compressive strength, respectively. At 6 kg/m^3, the corresponding values are numerically higher by 8.0%, 11.0%, 10.5%, and 3.1%. Each test group contained three specimens from one batch per dosage. Whether these differences exceed specimen variability requires the individual results and dispersion measures. The comparisons are descriptive, and between-batch reproducibility was not assessed.

Additional fiber-matrix interfaces or local microcracking may contribute to strength loss [13]. Conversely, fiber bridging may limit crack opening and indirectly restrain lateral dilation; an interconnected fiber network is another proposed interpretation [8]. These mechanisms were not demonstrated by the reported measurements. Variations in fiber dispersion, workability and entrapped air could also affect strength [8] [13]. The available dataset does not isolate these contributions or establish the cause of the decrease at 3 kg/m^3 and increase at 6 kg/m^3.

Table 4. Basic mechanical properties of BFRAC.

Test type	Basalt fiber dosage (kg/m^3)		
	0	3	6
Compressive strength (MPa)	31.21	29.14 (−6.6%)	33.72 (+8.0%)
Splitting tensile strength (MPa)	1.82	1.74 (−4.4%)	2.02 (+11.0%)
Flexural strength (MPa)	4.48	4.29 (−4.2%)	4.95 (+10.5%)
Axial compressive strength (MPa)	22.28	21.21 (−4.8%)	22.96 (+3.1%)

Figure 5 shows the photographed failure patterns after axial compression. The illustrated fiber-reinforced specimens appear to have narrower visible cracks and better retained integrity than the fiber-free specimen. These photographs provide qualitative observations for the specimens shown, rather than quantitative measurements of crack width or evidence of an internal fiber network. The observations are consistent with a possible crack-bridging contribution [8], but they do not directly establish internal stress redistribution, lateral confinement or the formation of fiber-induced microcracks.

3.2. Stress-Strain Relationship and Compressive Toughness

Figure 2 shows the reported compressive stress-strain responses. The peak stresses listed in Table 5 are 22.43, 20.40, and 24.43 MPa for RAC-0, RAC-3, and RAC-6, respectively. The fiber-reinforced curves show a more gradual descending branch over the plotted interval. The reported peak strains are 0.001950, 0.002050, and 0.002120. The strain at 50% of the peak stress on the descending branch, denoted ε50, is used as a deformation-capacity indicator and is 0.004485, 0.006660, and 0.008268, respectively. Relative to RAC-0, RAC-6 therefore has numerically larger peak strain and ε50 by 8.7% and 84.3%, respectively. The Table 5 values are averages based on three specimens per dosage. They were obtained from a separate group of prisms from the Table 4 axial-strength tests. The results are averages based on three stress-strain specimens per dosage. These specimens form a separate group from the three axial-strength specimens used for Table 4, although both groups have the same dimensions and batch source.

Table 5. Parameters of the reported BFRAC stress-strain responses.

Specimen type	Fiber dosage ($kg \cdot m^{-3}$)	Peak stress (MPa)	Peak strain	Strain at 0.5fp (ε50)
RAC-0	0	22.43	0.001950	0.004485
RAC-3	3	20.40	0.002050	0.006660
RAC-6	6	24.43	0.002120	0.008268

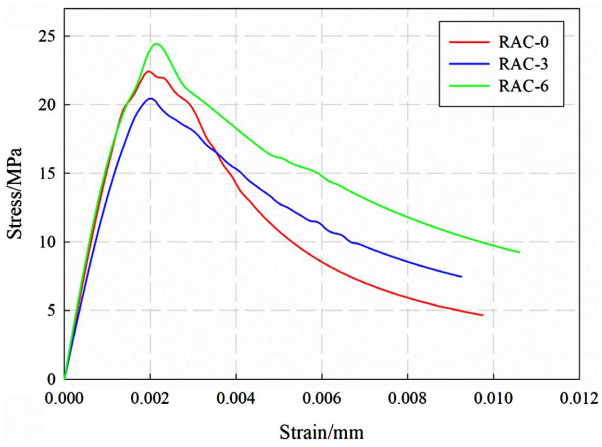


Figure 2. BFRAC stress-strain curves.

The curves were normalized using $x = \varepsilon/\varepsilon p$ and $y = \sigma/fp$, where εp and fp are the peak strain and peak stress of the relevant response. Figure 3 shows broadly similar ascending branches and flatter descending branches for the fiber-reinforced responses. Normalization describes curve shape but removes the absolute stress and strain scales; the area under a normalized curve is therefore not used as a substitute for compressive toughness calculated from the measured dimensional stress-strain records.

Compressive toughness is defined here as the area under a measured engineering stress-strain record over a common absolute-strain interval. For specimen i, $T_i(\varepsilon c) = \int_0^{\varepsilon c} \sigma_i(\varepsilon) d\varepsilon$. The same εc must be used for all included specimens; separate group-specific ε50 endpoints must not be used for this comparison.

Based on the stress-strain curves, the compressive toughness can be calculated. The compressive toughness of RAC-0, RAC-3 and RAC-6 were 2.27, 3.05 and 2.97, respectively. The compressive toughness of the fiber-reinforced specimens was significantly improved, with RAC-3 showing a 34.3% increase compared with RAC-0. This further indicates that the addition of fibers improves the crack resistance of concrete.

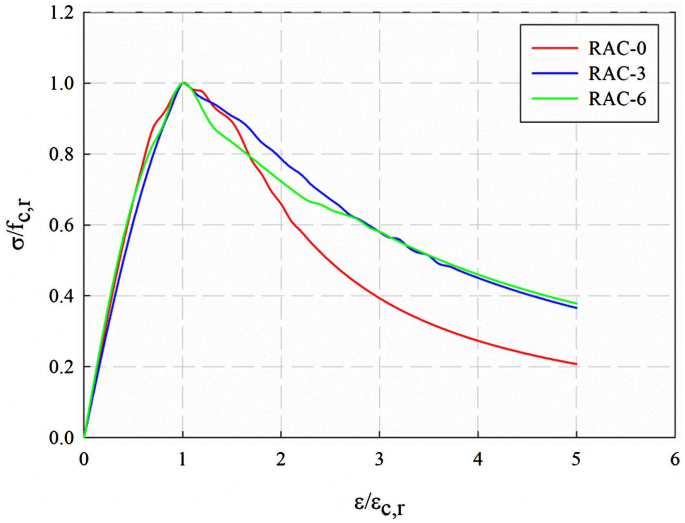


Figure 3. Normalized BFRAC stress-strain curves.

3.3. Constitutive Model for BFRAC

Establishing a concrete constitutive model is highly useful for nonlinear analysis and design. In this study, the measured curves were discretized and least-squares fitting was used to derive a uniaxial compressive stress-strain constitutive equation for BFRAC. The piecewise stress-strain equation proposed by Professor Zhenhai Guo [14] was adopted to fit the BFRAC constitutive model, as follows:

$$y = ax + (3-2a)x^2 + (a-2)x^3 \quad (x \le 1) \tag{1}$$

$$y = \frac{x}{b(x-1)^2 + x} \quad (x > 1) \tag{2}$$

Here, a and b are fitting parameters. Figure 4 compares fitted and experimental responses, and Table 6 lists the reported fit results. For the adopted normalized descending-branch equation, a smaller b gives a flatter branch. The reported b values decrease from 1.12678 to 0.66695 and 0.56572 across the three dosages. This is a description of the fitted response shape; it does not establish dissipated energy or prove that a fiber network formed. The possible mechanisms are discussed in Section 3.1.

Table 6. Parameters fitted to the reported stress-strain responses.

Specimen type	Ascending-branch parameters		Descending-branch parameters	
	a	R	b	R
RAC-0	1.36563	0.99956	1.12678	0.99613
RAC-3	1.34499	0.99988	0.66695	0.99285
RAC-6	1.35016	0.99771	0.56572	0.95005

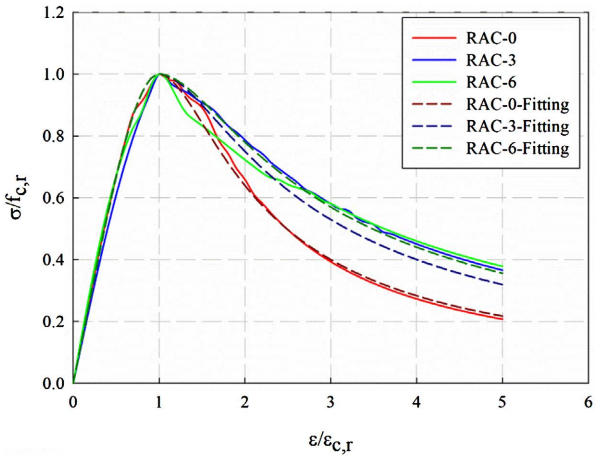


Figure 4. Fitted and experimental BFRAC stress-strain curves.

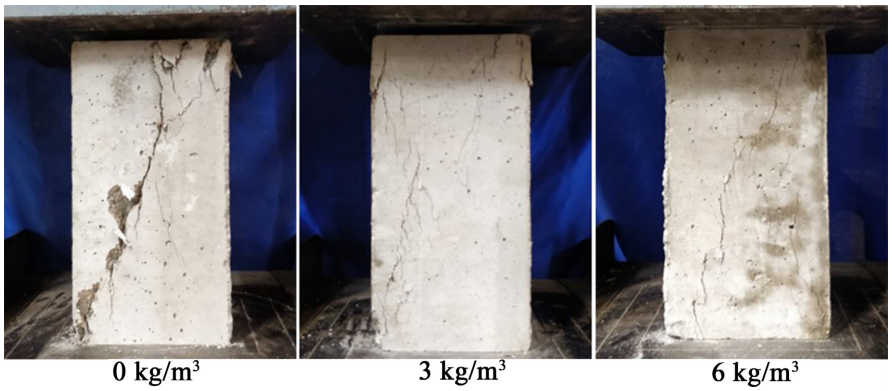


Figure 5. Failure modes of specimens after axial compression testing.

4. Conclusions

(1) With the incorporation of basalt fibers, the basic mechanical properties of

recycled aggregate concrete first decreased and then increased. At a basalt fiber dosage of 6 kg/m^3, all basic mechanical properties exceeded those of recycled aggregate concrete without fibers.

(2) Basalt fibers were particularly effective in improving the splitting tensile strength and flexural strength of recycled aggregate concrete. At a fiber dosage of 6 kg/m^3, these properties increased by 11.0% and 10.5%, respectively.

(3) The fiber-reinforced stress-strain responses showed a more gradual descending branch. For RAC-6, the peak strain and ε50 were numerically higher than for RAC-0 by 8.7% and 84.3%, respectively, suggesting greater deformation capacity.

Conflicts of Interest

The author declares no conflicts of interest regarding the publication of this paper.

References

[1] Liu, J., Guo, G., Wang, X., Lv, C., Wang, D. and Geng, H. (2025) Investigation of Mechanical Properties of Recycled Aggregate Concrete Incorporating Basalt Fiber, Copper Slag, and Ground Granulated Blast Furnace Slag. *Buildings*, **15**, Article 2214. https://doi.org/10.3390/buildings15132214

[2] Akbulut, Z.F. and Guler, S. (2026) Sustainable Recycled Aggregate Concrete Incorporating Volcanic Ash and Basalt Fibers with Enhanced Mechanical, Durability, and Environmental Performance. *ACS Omega*, **11**, 48050-48070. https://doi.org/10.1021/acsomega.6c04151

[3] Li, W., Xiao, J., Sun, Z. and Shah, S.P. (2012) Failure Processes of Modeled Recycled Aggregate Concrete under Uniaxial Compression. *Cement and Concrete Composites*, **34**, 1149-1158. https://doi.org/10.1016/j.cemconcomp.2012.06.017

[4] Malešev, M., Radonjanin, V. and Marinković, S. (2010) Recycled Concrete as Aggregate for Structural Concrete Production. *Sustainability*, **2**, 1204-1225. https://doi.org/10.3390/su2051204

[5] Bao, S., Wang, S., Xia, H., Liu, K., Tang, X. and Jin, P. (2025) Enhancing the Mechanical Properties of Recycled Aggregate Concrete: A Comparative Study of Basalt- and Glass-Fiber Reinforcements. *Buildings*, **15**, Article 1718. https://doi.org/10.3390/buildings15101718

[6] Shi, W., Guo, Y., Liu, Y., Wang, W., Duan, P., Bian, H., *et al.* (2024) Impact of Basalt Fiber on the Fracture Properties of Recycled Aggregate Concrete. *Construction and Building Materials*, **418**, Article 135363. https://doi.org/10.1016/j.conbuildmat.2024.135363

[7] Sim, J., Park, C. and Moon, D.Y. (2005) Characteristics of Basalt Fiber as a Strengthening Material for Concrete Structures. *Composites Part B*: *Engineering*, **36**, 504-512. https://doi.org/10.1016/j.compositesb.2005.02.002

[8] Guo, Y., Liu, Y., Wang, W., Wang, K., Zhang, Y. and Hou, J. (2023) Effect of Basalt Fiber on Uniaxial Compression-Related Constitutive Relation and Compressive Toughness of Recycled Aggregate Concrete. *Materials*, **16**, Article 1849. https://doi.org/10.3390/ma16051849

[9] Sun, S., Tai, H., Tan, Z. and Wei, C. (2025) Research on the Uniaxial Compression Performance of Basalt Fiber-Reinforced Recycled Aggregate Concrete. *Materials Science*, **32**, 451-459. https://doi.org/10.5755/j02.ms.41293

[10] Dong, J.F., Wang, Q.Y. and Guan, Z.W. (2017) Material Properties of Basalt Fibre Reinforced Concrete Made with Recycled Earthquake Waste. *Construction and Building Materials*, **130**, 241-251. https://doi.org/10.1016/j.conbuildmat.2016.08.118

[11] Katkhuda, H. and Shatarat, N. (2017) Improving the Mechanical Properties of Recycled Concrete Aggregate Using Chopped Basalt Fibers and Acid Treatment. *Construction and Building Materials*, **140**, 328-335. https://doi.org/10.1016/j.conbuildmat.2017.02.128

[12] GB 50081-2002 (2002) Standard for Test Method of Mechanical Properties on Ordinary Concrete. National Standard of the People's Republic of China.

[13] Tahwia, A.M., Helal, K.A. and Youssf, O. (2023) Chopped Basalt Fiber-Reinforced High-Performance Concrete: An Experimental and Analytical Study. *Journal of Composites Science*, **7**, Article 250. https://doi.org/10.3390/jcs7060250

[14] Guo, Z.H. (1997) Strength and Deformation of Concrete: Experimental Basis and Constitutive Relationships. Tsinghua University Press.